^{13}C-NMR, ^{1}H-NMR, and FT-Raman Study of Radiation-Induced Modifications in Radiation Dosimetry Polymer Gels

M. LEPAGE,[1] A. K. WHITTAKER,[2] L. RINTOUL,[3] C. BALDOCK[1]

[1] Centre for Medical and Health Physics, Queensland University of Technology, GPO Box 2434, Brisbane, Queensland 4001, Australia

[2] Centre for Magnetic Resonance, University of Queensland, Brisbane, Queensland 4072, Australia

[3] Centre for Instrumental and Developmental Chemistry, Queensland University of Technology, GPO Box 2434, Brisbane, Queensland 4001, Australia

Received 29 December 1999; accepted 7 April 2000

ABSTRACT: ^{1}H- and ^{13}C-NMR spectroscopy and FT-Raman spectroscopy are used to investigate the properties of a polymer gel dosimeter post-irradiation. The polymer gel (PAG) is composed of acrylamide, *N*,*N*′-methylene-bisacrylamide, gelatin, and water. The formation of a polyacrylamide network within the gelatin matrix follows a dose dependence nonlinearly correlated to the disappearance of the double bonds from the dissolved monomers within the absorbed dose range of 0–50 Gy. The signal from the gelatin remains constant with irradiation. We show that the NMR spin–spin relaxation times (T_2) of PAGs irradiated to up to 50 Gy measured in a NMR spectrometer and a clinical magnetic resonance imaging scanner can be modeled using the spectroscopic intensity of the growing polymer network. More specifically, we show that the nonlinear T_2 dependence against dose can be understood in terms of the fraction of protons in three different proton pools. © 2000 John Wiley & Sons, Inc. J Appl Polym Sci 79: 1572–1581, 2001

Key words: polymer gel; dosimetry; magnetic resonance imaging; NMR; FT-Raman

INTRODUCTION

In clinical radiotherapy there is a requirement to measure 3-dimensional (3-D) radiation dose distributions. This is particularly important in situations where high dose gradients exist and where it is necessary to verify dose distributions calculated by 3-D treatment planning computers. Common dosimeters (i.e., ionization chambers, thermoluminescent diodes, radiographic films, etc.) do not allow the measurement of 3-D dose distributions because of severe spatial limitations.[1]

In 1984 it was proposed to use NMR relaxation measurements of the Fricke[2] ferrous sulfate dosimeter.[3] Ionizing radiation causes ferrous (Fe^{2+}) ions to be converted to ferric ions (Fe^{3+}) through radiolysis of an aqueous gel system. Fe^{3+} ions exhibit a larger paramagnetic enhancement than Fe^{2+} ions, and the NMR spin–lattice (T_1) and spin–spin (T_2) relaxation times of the dosimeter are related to the concentration of Fe^{3+} produced and hence to the absorbed radiation dose. In this radiation dosimetry system, ferrous sulfate solutions were incorporated into a gel matrix in order to spatially stabilize the absorbed dose signature. Dose maps can be obtained using magnetic resonance imaging (MRI). A limitation in ferrous sulfate dosimetry systems is the diffusion of ions in

Correspondence to: C. Baldock (c.baldock@qut.edu.au).
Contract grant sponsor: Queensland Cancer Fund.

Journal of Applied Polymer Science, Vol. 79, 1572–1581 (2001)

the dosimeter, resulting in a spatially unstable relaxation time or rate distribution.[4–10]

Dosimetry based on the radiation-induced chemical changes in polymers was suggested in 1954.[11] As a result, the change in viscosity of polyacrylamide solutions, which was supposedly proportional to the absorbed dose of radiation, was proposed as a dosimeter in 1961.[12] More recently, polyacrylamide gel (PAG) radiation dosimeters were proposed in which the copolymerization of acrylamide (AA) and *N*,*N*′-methylene-bisacrylamide (BIS) monomers is believed to take place. The monomers and final products are retained in a gel matrix of either agarose or gelatin.[13,14] In these radiologically tissue equivalent polymer networks,[15,16] the crosslinking of the monomers was suggested to increase during the copolymerization process in proportion to the absorbed radiation dose, although the final products were not identified. Nevertheless, the resulting change in the T_2 could be monitored using NMR relaxation measurements. The uses of PAG for radiotherapy dosimetry applications were reported.[17–24] In addition to MRI,[13,23] optical techniques including FT-Raman,[25] laser attenuation,[26] and X-ray computed tomography[27] can also be used to monitor the changes in PAG dosimeters upon irradiation.

Despite the great clinical potential of gel dosimetry, it is probably fair to say that no clinical radiotherapy treatment has been altered because of the results of gel dosimetry. This is partly due to a lack of understanding of the fundamental processes taking place in these materials post-irradiation. The chemical modifications occurring in PAGs have not been ascertained, leaving unanswered the fundamental questions concerning the behavior of the changes in NMR relaxation times after irradiation with ionizing radiation. Consequently, there is a good deal of confusion in the existing literature where heuristic conclusions have been drawn without firm experimental evidence. This lack of knowledge results in unacceptably large uncertainties in the evaluation process. It is therefore necessary to undertake fundamental measurements on these materials to be able to develop gel dosimeters that will be of use in the field of radiation oncology.

Various techniques can be employed to obtain information on the chemical changes occurring at a molecular level. For example, NMR spectroscopy and FT-Raman have the potential to provide quantitative information on the presence of different chemical groups in a molecule.

We measured the ^{13}C-NMR, ^{1}H-NMR, and FT-Raman spectra of a PAG dosimeter with the view to relating the macroscopic parameter T_2 to microscopic radiation-induced modifications in the system. The polymer gel consists of two monomers (AA and BIS) dissolved in an aqueous gelatin matrix. The measurements were performed on different samples having absorbed doses up to 50 Gy. The results provide evidence for the polymerization of the monomers that form a polyacrylamide network within the gelatin matrix. We show that the T_2 of irradiated samples, measured with a NMR spectrometer and with an MRI scanner, can be modeled using the number of protons of the growing polyacrylamide network derived from FT-Raman spectroscopy. The latter calculations draw a direct link between the experimental observations of a growing polymer network and the associated changes in the T_2 recorded with clinical MRI scanners.

EXPERIMENTAL

NMR Spectroscopy and Relaxation Time Measurements

The NMR measurements were performed with a Bruker MSL-300 spectrometer operating at a frequency of 300.13 MHz for ^{1}H and 75.482 MHz for ^{13}C. The spectrometer was equipped either with a commercial 7- or 4-mm double air bearing, magic angle spinning probe, or a static 7-mm double resonance probe. Unless otherwise indicated, the samples were spun at approximately 1.5 kHz to provide partial averaging of the dipolar couplings, as well as averaging over B-field distortions.[28] The 90° pulse time for ^{1}H-NMR was 6 μs, the spectrum width was 5 kHz, and 8000 data points were acquired. The 90° pulse time used in the high power proton-decoupled single pulse ^{13}C spectra was 5.5 μs. The spectrum width was 38 kHz, and 4000 data points were acquired.

The chemical shift scale of the ^{1}H-NMR spectra followed the arbitrary setting of the H_2O peak to 4.9 ppm while that of the ^{13}C spectra was referenced to the low-field resonance of adamantane (38.23 ppm). The samples were left to equilibrate at room temperature (22°C), transferred in ZrO_2 rotors, and immediately scanned.

The T_2 measurements were performed using the Carr–Purcell–Meiboom–Gill sequence. A single point was collected at the echo maximum for 1024 echoes in a pulse train. The time between successive 180° pulses was varied from 1.2 to 6.0

ms to optimize the recording for our samples having a range of T_2 values from 200 ms to 2 s, respectively. In each case, the final intensity was less than 5% of the original intensity. This condition ensured reliable exponential fits to the data.

The T_2 measurements were also undertaken using the head coil of a Siemens Vision MRI scanner operating at a frequency of 64 MHz. The sample temperature was approximately 21°C. A container holding the vials of gel was imaged with a single slice in the coronal (horizontal) plane using a modified conventional 32 echo spin–echo pulse sequence. A repetition time of 4000 ms and repeated echoes with an echo spacing of 50 ms was used. The field of view was 256 × 256 mm, the slice thickness was 5 mm, and the pixel size was 1.0 × 1.0 mm. Four signal acquisitions were used. Data were subsequently transferred to a personal computer and processed to calculate T_2 image "maps" using software written in-house.[29] Regions of interest of similar area and number of pixels were drawn on each vial in the map to obtain the T_2 values.

FT-Raman Spectroscopy

A complete description of the FT-Raman spectrometer (2000 FT-Raman spectrometer system, Perkin–Elmer, Beaconsfield, UK) used here was reported previously.[25] Briefly, the beam from a continuous wave Nd:yag laser emitting at 1064 nm is directed onto the samples and the scattered radiation is detected with an InGaAs detector. There were 250 acquisitions at a resolution of 8 cm^{-1}, and a laser power of 400 mW recorded for each sample.

Sample Preparation

The samples were prepared in a glove box purged with N_2. Oxygen is known to have an inhibitory effect on the free-radical chemistry of irradiated liquids[30] and on free-radical polymerization.[31] More specifically, O_2 was shown to rapidly react with acrylamide radicals.[32] For this reason, the atmosphere inside the glove box contained less than 0.2 ppm of O_2, as measured with an oxygen meter (Quest Technologies). The samples for NMR spectroscopy and FT-Raman spectroscopy were kept in sealed "P6" glass vials (Amersham International) prefilled with N_2. The samples to be imaged in the MRI scanner were kept in screw-top glass vials. The samples were made of AA (99+%, electrophoresis grade, Aldrich), BIS (99+%, electrophoresis grade, Aldrich), gelatin (300 bloom, Aldrich), and H_2O (deionized) or D_2O (99.9+% D atom, Aldrich). The details of the manufacture of the gels were described previously.[23] The polymer gel used in this study consisted of 3% AA, 3% BIS, 5% gelatin, and 89% H_2O by weight. This formulation was previously given the acronym PAG,[23] which is loosely used here, even for our samples containing D_2O instead of H_2O.

The samples were irradiated at 22°C with γ photons from ^{60}Co in a Gammacell 200 (Atomic Energy Canada Limited). Typically, the samples irradiated to 1 and 2 Gy were placed in a lead attenuator and the dose rate was 0.06 Gy s^{-1}. Otherwise, the samples were placed in a polystyrene holder and the dose rate was 0.27 Gy s^{-1}. Both dose rates were calibrated with an ion chamber.[33] A comparison between two gels irradiated to 10 Gy at one or the other dose rate showed no detectable difference in the T_2 values. Because the T_2 evolves rapidly in the first few hours following irradiation, and more slowly thereafter,[34,35] the samples were left in a refrigerator for at least 3 days prior to the NMR investigations.

Degradation Model

Consider a target, containing initially n_0 reactant molecules, that absorbs a differential dose D. In a polymerization reaction, the rate of polymerization is proportional to the number of reactant molecules[36] and a first order process is expected. The number of reactant molecules n_D remaining after the absorption of a dose D is

$$n_D = A + n_0 e^{-D/C} \quad (1)$$

where A is a parameter introduced to take into account the background intensity underlying a considered feature in a spectrum. The overall shape of the curve is an exponential decay with an initial intensity $A + n_0$ and the final intensity is A. If we remove the background intensity from a spectrum, the dose constant C can be redefined as a half-dose, $D_{1/2} = 0.693C$, which is simply the dose required to obtain half the initial number of molecules.

RESULTS

Peak Assignments

With the present formulation, the water protons accounted for about 91.9% of the total number of protons. Hence, the ^1H-NMR spectra were highly

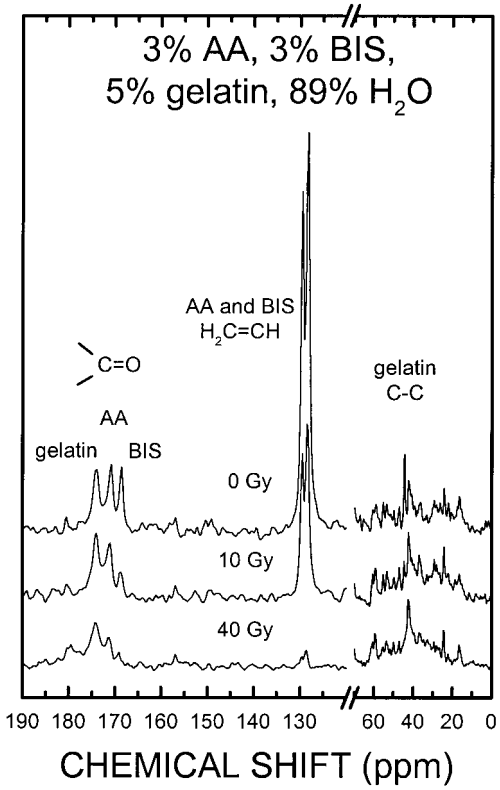

Figure 1 ^{13}C-NMR spectra at 75.482 MHz of a PAG. The spectra for the samples having absorbed doses of 0, 10, and 40 Gy are shifted for clarity. The structures ascribed to the C═C double bonds of AA and BIS decrease with the absorbed radiation dose.

dominated by the water signal. Replacing H_2O with D_2O lowered the water signal. It was then possible to increase the receiver gain and thus obtain a better signal to noise ratio for the weaker peaks without extending the measurement time. Figure 1 shows the ^{13}C-NMR spectra of a PAG dosimeter irradiated at 0, 10, and 40 Gy. Figure 2 shows ^{1}H-NMR recorded at 300.13 MHz for PAGs irradiated at 0, 10, and 50 Gy. The peaks were assigned in comparison with spectra recorded from separate aqueous solutions of the chemicals diluted in H_2O and D_2O. A similar procedure was used in an independent measurement of the ^{1}H spectrum of an unirradiated gel and the peak assignments were identical.[37] Some structures in the ^{1}H spectrum of polyacrylamide may be influenced by the solvent, the pH, and the temperature.[38] However, the assignments were in agreement with published spectra of polyacrylamide.[39,40] ^{1}H-NMR spectra were reported for AA and BIS in solution, and the relative position of the peaks was similar.[41]

In the ^{13}C spectra (Fig. 1), a doublet near 129 ppm was specifically assigned to the vinyl groups of AA and BIS. Numerous peaks were found between 0 and 80 ppm and these could be attributed to gelatin, which incidentally is composed of 20 or more different monomeric species.[42] From the separate measurements on individual aqueous solutions of AA and BIS, we identified the following structures between 166 and 183 ppm. The signal from the carbonyl group of BIS was located at 168.6 ppm while that of AA was at 170.8 ppm. The spectrum from gelatin contained several peaks located at 171, 174.5, 177.4, 181.6, and 184.7 ppm. In the polymer gel system including AA, BIS, and gelatin, all these peaks were superimposed. In the same spectral region, the high resolution ^{13}C of polyacrylamide from Ganapathy et al. showed a single narrow peak assigned to the carbonyl carbon at about 175 ppm.[40]

In the ^{1}H spectra of Figure 2 the dominant peak near 4.9 ppm was attributed to residual H_2O and HDO molecules. We note that the intensity of this peak was 3.5% of the water peak when H_2O

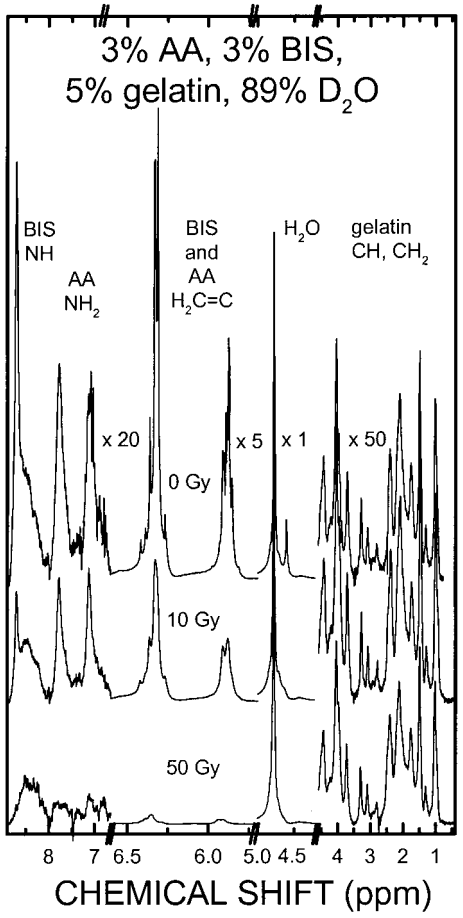

Figure 2 ^{1}H-NMR spectra at 300.13 MHz of a PAG. The spectra for the samples having absorbed doses of 0, 10, and 50 Gy are shifted for clarity.

was used. At the foot of this peak, a small peak located at 4.8 ppm was attributed to the central CH_2 group of BIS. A second set of experiments was performed on three samples containing H_2O having absorbed 0, 10, and 50 Gy. The samples were spun at 6 kHz to prevent the spinning side bands from overlapping the structures. The results are shown in Figure 2 for the chemical shift range from 6.65 to 8.9 ppm. A doublet having peaks located at 7.1 and 7.8 ppm was assigned to the inequivalent protons of the NH_2 group of AA. A peak centered at 8.7 ppm, attributed to the NH groups of BIS, was superimposed on a broad signal attributed to the NH groups of gelatin. A ^{1}H-NMR study of the amide side chain of a commercial polyacrylamide sample revealed a triplet centered near 7.7 ppm and a singlet at about 7 ppm that were assigned to the trans and cis proton of the amide group, respectively.[38] Two sharp multiplets observed near 5.9 and 6.3 ppm were assigned to the vinyl groups of AA and BIS. The large number of peaks recorded between 0 and 4.65 ppm were attributed to gelatin. We observed new peaks at 2.3 and 1.8 ppm from solutions of AA in H_2O irradiated at 50 Gy (not shown). The latter, which may have been due to CH_2 groups of a polyacrylamide network, were not seen in the spectra of the irradiated polymer gel of Figure 2.

A set of FT-Raman spectra recorded from PAG samples having absorbed up to 50 Gy was reported earlier.[25] However, we acquired a new set of spectra in order to get a better signal to noise ratio to analyze structures having low intensities.

Figure 3 shows a portion of the FT-Raman spectra of the polymer gel between 2800 and 3150 cm^{-1} for three different absorbed doses of 0, 10, and 50 Gy. The 0-Gy spectrum contains two prominent peaks with maxima at 3111 and 3039 cm^{-1}, as well as structures at 2995, 2980, 2940, and 2884 cm^{-1}. The first two were ascribed to the antisymmetric and symmetric vinyl CH stretch from both BIS and AA. The peak at 2995 cm^{-1} was ascribed to the alkyl CH stretch of AA. The intensity of the peaks at 2940, 2980, and 2884 cm^{-1}, although different from zero in the 0-Gy spectrum, increased with the absorbed dose. The peaks at 2940 and 2884 cm^{-1} resulted from the excitation of the antisymmetric and symmetric alkyl CH stretches from gelatin and, as is discussed below, from a growing polymer network. The 2980 cm^{-1} band was attributed to the CH group part of a polymer chain.

Finally, we recall that two bands located at 1256 and 1285 cm^{-1} were previously assigned to the vinyl δ_{CH_2} vibrations of BIS and AA, respectively.[25] The intensity of the vinyl δ_{CH_2} vibrations was dependent on the absorbed dose and thus FT-Raman imaging was proposed to obtain dose distributions with high spatial resolution.[25]

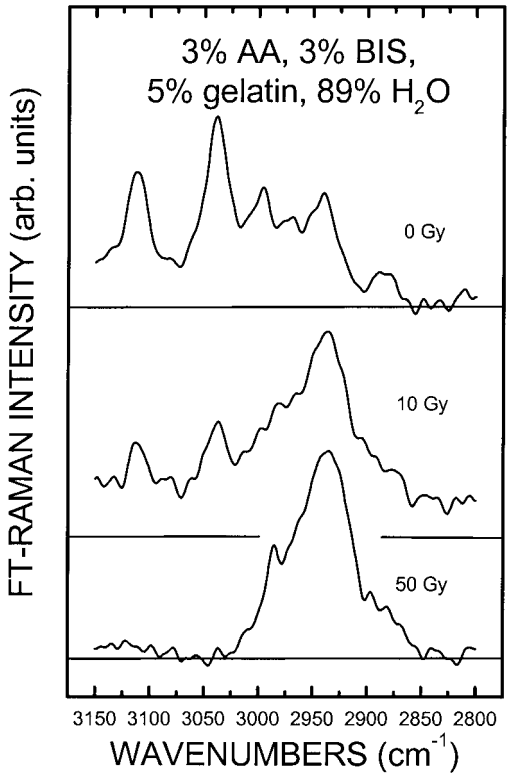

Figure 3 FT-Raman spectra between 2800 and 3150 $cm^{-1}$of a PAG for three different absorbed doses of 0, 8, and 50 Gy, which are shifted vertically for clarity. On the 0-Gy spectrum, two prominent peaks are seen at 3111 and 3039 cm^{-1}. They are ascribed to the antisymmetric and symmetric vinyl CH stretch from both BIS and AA. Although their intensity decreases with the absorbed dose, the intensity of the 2980 and the 2884 cm^{-1} peaks increases. They are specifically ascribed to the antisymmetric and symmetric alkyl CH stretches of a growing polyacrylamide network.

Peak Intensities as Function of Absorbed Dose

The water content of the samples did not change significantly with the absorbed dose. Assuming a G value of 5 for the dissociation of water molecules,[43] only 4.7×10^{-7}% of the H_2O molecules will be broken after a 50-Gy absorbed dose. Furthermore, the signal from water vibrations in all FT-Raman spectra was found to be constant over the absorbed dose range studied. Therefore, the intensity scales of the different ^{1}H spectra recorded for samples having absorbed from 0 to 50 Gy were normalized to the residual water peak

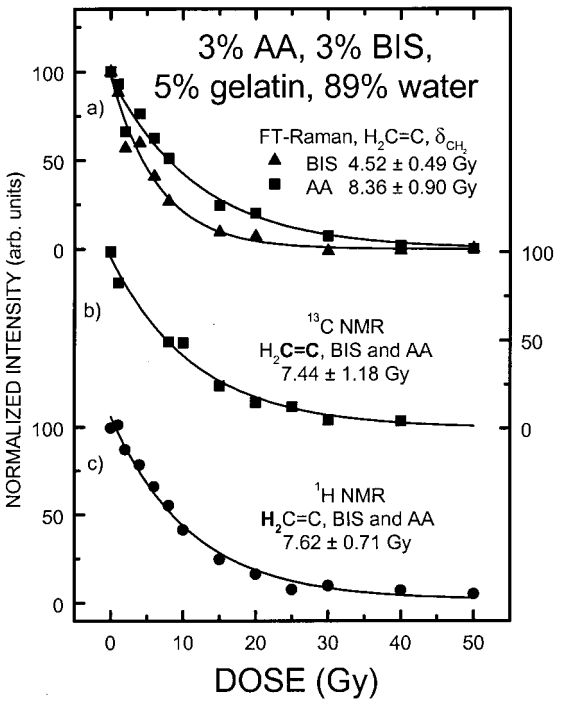

Figure 4 A comparison of the intensity of the —C═CH_2 vinyl (δ_{CH_2}) vibrations of AA and BIS with the ^{1}H- and ^{13}C-NMR signal from the same chemical moiety. The PAGs are composed of 3% AA, 3% BIS, 5% gelatin, and 89% H_2O by weight in the FT-Raman (curve a) and ^{13}C-NMR (curve b) results and 89% D_2O in the ^{1}H-NMR results (curve c). The half-doses from the monoexponential fits are discussed in the text.

intensity. By comparing the ^{1}H spectra at different doses, it was apparent that the peaks assigned to gelatin (0–4.65 ppm) remained unchanged upon irradiation while those ascribed to the vinyl group of AA and BIS decreased to zero. The ^{13}C spectra were therefore normalized to the integral of the signal originating from the gelatin peaks (0–80 ppm). It was then apparent that the peaks from the vinyl groups of AA and BIS decreased dramatically.

Figure 4 shows the integral of peaks assigned to various AA and BIS groups. The half-dose of the monoexponential fits to the data are also shown in the figure. More specifically, the curves were fitted with the exponential decay function of eq. (1). We used a built-in monoexponential fitting function based on the Levenberg–Marquardt algorithm from Microcal™ Origin™ (Microcal Software, Inc., Northampton, MA), which gives the value and the absolute uncertainty of the parameters that best describe the data.

The vinyl δ_{CH_2} vibrations of BIS and AA were observed at 1256 and 1285 cm^{-1}, respectively, with FT-Raman spectroscopy.[25] Those bands decayed exponentially with the absorbed dose, although with a different half-dose (Fig. 4, curve a). More specifically, the half-doses of the exponential decays for AA and BIS were 8.36 ± 0.90 and 4.52 ± 0.49 Gy, respectively. A similar observation confirming the faster disappearance of BIS was reported by Nieto et al. for the chemically induced copolymerization of AA and BIS in solution and was taken as evidence for the larger reactivity of BIS.[41]

Figure 4 represents the intensity of the peaks assigned to the vinyl groups of AA and BIS located near 129 (curve a) and 5.9 ppm (curve b) in the ^{13}C and ^{1}H spectra, respectively. The half-doses were 7.44 ± 1.18 and 7.62 ± 0.71 Gy, respectively. The spectroscopic signature of the vinyl groups of AA and BIS are superimposed in our ^{13}C- and ^{1}H-NMR spectra. By simply weighting the half-doses for AA and BIS obtained from FT-Raman by the total number of double bonds, we obtained a half-dose of 6.52 ± 0.70 Gy. Considering that the errors quoted only include the uncertainty from the fitting procedure, the agreement between the estimated weighted value and the experimentally determined values was very good. This justified the normalization of the NMR spectra a posteriori and showed the good agreement between the two spectroscopic approaches.

The main features in the region of the FT-Raman spectra located between 2850 and 3150 cm^{-1} (Fig. 3) can be reasonably well fitted with 6 Gaussians centered at the locations mentioned above. The intensity of the bands located at 3111, 3039, 2940, and 2884 cm^{-1} are shown in Figure 5. The first two bands were found to have respective half-doses of 7.28 ± 1.62 (═CH_2 antisymmetrical stretch, BIS and AA) and 6.63 ± 0.53 Gy (═CH_2 symmetrical stretch, BIS and AA). On the other hand, the bands located at 2940 and 2884 cm^{-1} were growing with the absorbed dose with respective half-doses of 6.20 ± 1.81 and 5.37 ± 2.15 Gy. The relatively large uncertainty on the latter half-dose value stemmed directly from the relatively low signal intensity of the band located at 2884 cm^{-1} (Fig. 3).

Spin–Spin Relaxation Time for Different Absorbed Doses

Figure 6 shows the T_2 measured from PAG dosimeters that absorbed up to 50 Gy, which were measured with the 300.13-MHz NMR spectrometer and 64-MHz clinical MRI scanner. A tentative exponential fit to the data gave half-doses of 4.68

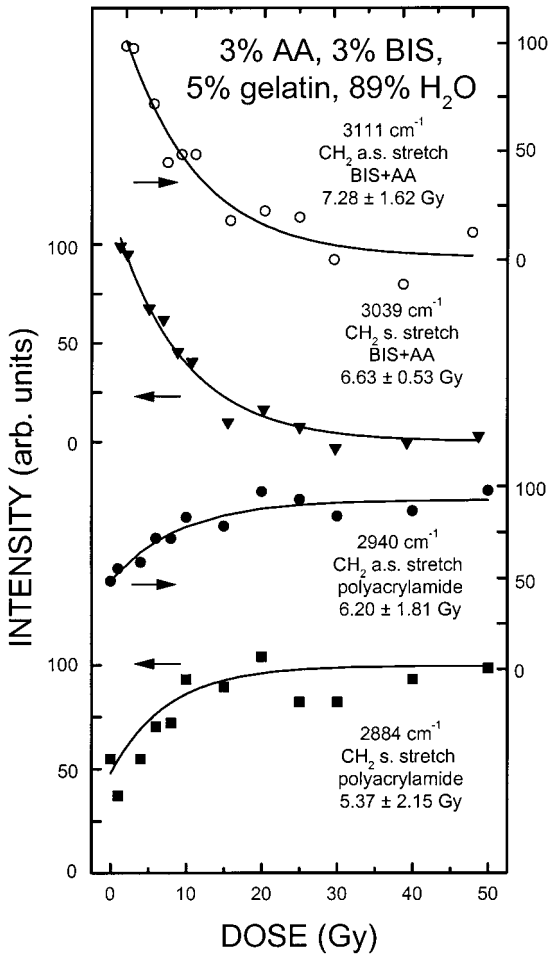

Figure 5 The intensity of the C—H stretching vibrations of AA, BIS, and a polyacrylamide network in a PAG as a function of the absorbed dose. The vibrations from the polyacrylamide network grow with the same half-dose as the vibrations from the monomers decay.

± 0.37 and 2.56 ± 0.06 Gy, respectively. The solid lines were obtained from a model described below. Also shown in Figure 6 are the commonly employed "dose response" [i.e., relaxation rate R_2 ($1/T_2$) against dose] graphs.

DISCUSSION

In the presence of a chemical initiator, AA and BIS are well known to form a polyacrylamide network in an aqueous solution.[44–47] Copolymerization of the vinyl groups of the monomers (AA and BIS) creates a C—C chain with amide side chains. BIS acts as a crosslinker that binds two chains together. The creation of clusters of finite size leads to an increased turbidity in polyacrylamide gels (PAGs).[47]

Our ^{1}H-NMR spectrum of an irradiated solution of AA (not shown) was very similar to the spectrum of a polyacrylamide sample published by Ganapathy et al.[40] This showed that radiation-induced polymerization of AA was achievable within the dose range used in this study. However, in a gelatin matrix, although the intensity of the double bonds from AA and BIS decreases rapidly with dose, the characteristic signature of the CH and CH_2 groups did not emerge from the gelatin background intensity. If we assume that copolymerization occurred (as evidenced below), the polyacrylamide chains crosslinked with BIS were likely to precipitate out of solution. As the quantity of polymer increased with the absorbed dose, the relaxation via interaction with the polymer surface became more efficient and the T_2 of this polymer gel dropped rapidly[13] (Fig. 6). The line width of the NMR peaks of the polymer is

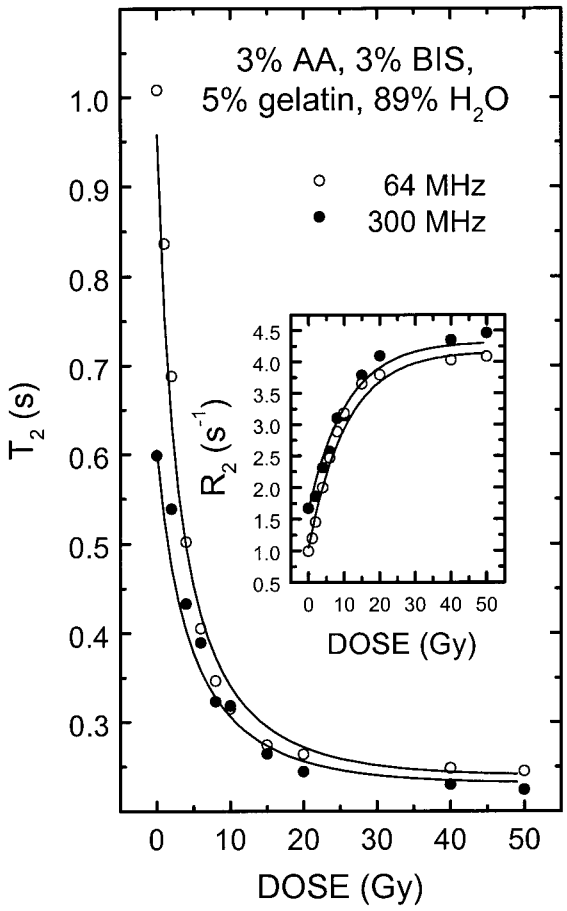

Figure 6 The nuclear spin–spin relaxation time (T_2) and relaxation rate (R_2) for PAG samples in the 0–50 Gy range. The results were obtained at (○) 64 and (●) 300.13 MHz. (—) The results as obtained with a model described in the text.

likely to become so broad that the peak will become very difficult to observe at room temperature, as was shown to be the case for the copolymerization of AA and BIS in solution.[39] It can thus be expected that the signal from other chemical groups in AA and BIS would "disappear" with the same half-dose as the double bonds. Cross-polarization (CP) experiments, on another hand, are more sensitive to the presence of rigid polymer chains. We measured the CP spectrum for the samples having absorbed 0 and 50 Gy. The latter showed the presence of a peak located at 41 ppm and a shoulder near 35 ppm. These peaks correspond to CH and CH_2 groups of polyacrylamide.[40,48,49]

The FT-Raman results of Figure 5 clearly show the formation of alkyl CH_2 vibrations, which indicates the formation of a saturated chain of carbon atoms. Within the uncertainties in the fits, the half-dose for the appearance of the alkyl CH_2 vibrations was the same as for the disappearance of the double bonds. Furthermore, the value of the half-dose was confirmed by both the ^{1}H- and ^{13}C-NMR results (Fig. 4).

In Bansil and Gupta's[47] Raman study a band at 3045 cm^{-1} was observed that grew as copolymerization of AA and BIS in water proceeded. This vibrational band was assigned to a CH_2 stretching from a C═CH_2 group from a BIS molecule part of a polymer chain, but having one double bond unreacted. In the present study the intensity of this band was below the limit of detectability in Figure 3. Other researchers made a direct correlation between the amount of crosslinker (BIS) and the degree of crosslinking in a PAG.[50] However, the observation that some BIS molecules in polyacrylamide may have an unreacted double bond argues against such a direct relationship.

We obtained different G values (defined as the number of molecules of material changed, or of product formed, for each 100 eV of absorbed energy in the system[43]) from the NMR spectra and FT-Raman spectra. To a first approximation, the initial decrease of the double bonds intensity can be considered linear from 0 to 8 Gy. We observed that 50% of the double bond intensity from AA and 27% of that of BIS remained after 8 Gy. Knowing the initial chemical composition of the polymer gel, we calculated the G values for the consumption of the double bonds of AA to be $G(-db) = 2.54 \times 10^5$ and for BIS to be $G(-db) = 3.42 \times 10^5$. From those values, assuming every double bond of AA and BIS participates in the formation of an alkyl chain (i.e., copolymerization), the G value for the formation of alkyl CH_2 groups was calculated to be about $G(—CH_2—) = 5 \times 10^5$.

In a diluted solution, the initiation of polymerization is thought to be caused by free radicals of water. Therefore, if we make the crude assumption that every radical from water [G (total radical) ≈ 10][43] attacks a double bond from AA or BIS to initiate a polymerization reaction, we find that the degree of polymerization (i.e., the number of repeating monomer units in a polymer chain[31]) is of the order of 10^4, the same order of magnitude expected for vinyl polymerization[31] and that obtained for copolymerization of AA and BIS in solution.[51] The simple degradation model we used assumes a probability of reaction of a double bond with a water radical that is independent of the amount of polymer formed (i.e., independent of the remaining number of double bonds). The monoexponential decrease of the double bond intensity with the absorbed dose may suggest that this condition is realized in PAG dosimeters. This may imply that the diffusion of the monomers in the gelatin matrix is independent of the absorbed radiation dose, within the range covered in this study, in agreement with monomer diffusion measurements on the same system.[37]

Copolymerization reactions of AA and BIS create a solid polyacrylamide network within the gelatin matrix. We made calculations using the classic model of fast exchange[52] in which the measured T_2 is given by

$$\frac{1}{T_2} = \frac{f^H_{\text{mob}}}{T_{2,\text{mob}}} + \frac{f^H_{\text{pol}}}{T_{2,\text{pol}}} + \frac{f^H_{\text{gela}}}{T_{2,\text{gela}}} \qquad (2)$$

where f^H_{mob}, f^H_{pol}, and f^H_{gela} are the fraction of protons in the mobile, polymer, and gelatin pools, respectively; and $T_{2,\text{mob}}$, $T_{2,\text{pol}}$, and $T_{2,\text{gela}}$ are their respective intrinsic NMR spin–spin relaxation times. The fractions of protons in the first two pools were evaluated using the initial concentrations of the solution and the curve for the production of polymer CH_2 vibrations in Figure 5. The mobile pool initially contained the protons from water and the monomers, the latter protons being transferred with a half-dose of 7.50 Gy in the polymer pool. The fraction of gelatin protons was estimated to be 4.35% and was kept constant as suggested by Figures 1 and 2. Using a similar equation, the $T_{2,\text{gela}}$ could be determined experimentally to be 37 ms from a sample containing 5% gelatin and 95% H_2O. In order to fit the data, the $T_{2,\text{pol}}$ was set at 13 ± 1 ms and $T_{2,\text{mob}}$ was set at

2 s for 300.13 MHz. For comparison, the results obtained from the clinical MRI scanner operating at 64 MHz were added to Figure 6. The $T_{2,\mathrm{mob}}$ was set at 3 s, which agreed with the observation of an increase for T_2 with decreasing field strength for a polymer gel.[13] The results are presented as solid lines in Figure 6, and it is apparent that the relaxation properties of the PAG are well represented by the model.

On the basis of this simple model, it is not strictly correct to fit a monoexponential decay to the decrease in T_2 with the absorbed dose. However, the half-dose that was obtained from the 300-MHz measurements was 4.68 ± 0.37 Gy. Interestingly, this value is smaller than the half-dose used to calculate the number of protons in the polymer chain. Several authors simply assumed that the observed changes in T_2 were solely due to the "presence" of the solid formed polymer that was thought to increase linearly with the absorbed dose.[13,35,50,53] Although it may be approximated to a linear function in the first few Grays of radiation, the present work showed that there was no linear relationship between the increase in polymer protons and the decrease of T_2 (or the increase of R_2). Furthermore, the nonlinearity of T_2 (or R_2) with the absorbed dose has profound implications in the determination of the absorbed dose from the polymer gels in applied radiotherapy gel dosimetry.[54,55]

A recent article presented a study of the evolution of T_2 as a function of postirradiation time and showed a continuous decrease over many days.[35] Although the authors did not characterize the processes involved or the products formed and their affirmation was solely based on T_2 measurements, they claimed a polymerization reaction was proceeding throughout the time interval. We point out that a continuous phase separation or a rearrangement of the polymer giving it a tighter structure could also have a similar effect. We will address this issue in more detail in a forthcoming article.[56] We gathered some evidence that the T_2 relaxation is dominated by chemical exchange.[57] In this regard, not all amide protons in the polyacrylamide chain may be easily accessed for exchange, especially in the formation of complex geometries.

CONCLUSIONS

We characterized the chemical changes occurring in a PAG radiation dosimeter, consisting of AA, BIS, gelatin, and water, using ^{13}C-NMR, ^{1}H-NMR, and FT-Raman spectroscopy. We showed that irradiation of AA and BIS in a gelatin matrix leads to copolymerization of the monomers, without the inclusion of gelatin molecules. Specifically, the double bonds from AA and BIS disappeared with a half-dose near 7.5 Gy while the signal from gelatin remained constant over the absorbed dose range up to 50 Gy. A polyacrylamide network grew with the same half-dose, within experimental errors. This polyacrylamide network within the gelatin matrix was characterized with CP experiments results identical to a similar experiment performed on a polyacrylamide sample.[40] The T_2 values recorded at 64 and 300.13 MHz were fitted accurately by a simple classical model. The number of protons belonging to the polymer proton pool was directly derived from the FT-Raman spectra. Based on this model, new gel formulations covering a selected range of T_2 values can be envisaged.

The authors acknowledge P. J. Murry and P. M. Jayasekera for help provided in the manufacture of the gels. We thank D. J. T. Hill and J.-P. Jay-Gérin for useful discussions. We also thank Southern X-ray Clinics, Wesley Hospital, Brisbane, for access to their MRI facility.

REFERENCES

1. Schreiner, L. J., Ed. Proceedings of the 1st International Workshop on Radiation Therapy Gel Dosimetry; Canadian Organization of Medical Physicists: Edmonton, Canada, 1999.
2. Fricke, H.; Morse, S. Am J Roent Radium Ther Nucl Med 1927, 18, 430.
3. Gore, J. C.; Kang, Y. S.; Schulz, R. J. Phys Med Biol 1984, 29, 1189.
4. Schulz, R. J.; deGuzman, A. F.; Nguyen, D. B.; Gore, J. C. Phys Med Biol 1990, 35, 1611.
5. Olsson, L. E.; Westrin, B. A.; Fransson, A.; Nordell, B. Phys Med Biol 1992, 37, 2243.
6. Balcolm, B. J.; Lees. T. J.; Sharp, A. R.; Kulkarni, N. S.; Wagner, G. S. Phys Med Biol 1995, 40, 1665.
7. Baldock, C.; Harris, P. J.; Piercy, A. R.; Patval, S.; Prior, D. N.; Keevil, S. F.; Summers, P. Med Phys 1995, 22, 1540.
8. Harris, P. J.; Piercy, A. R.; Baldock, C. Phys Med Biol 1996, 41, 1745.
9. Kron, T.; Jonas, D.; Pope, J. M. Magn Reson Imaging 1997, 15, 211.
10. Pedersen, T. V.; Olsen, D. R.; Skretting, A. Phys Med Biol 1997, 42, 1575.
11. Alexander, P.; Charlesby, A.; Ross, M. Proc R Soc A 1954, 223, 392.
12. Boni, A. L. Radiat Res 1961, 14, 374.

13. Maryañski, M. J.; Gore, J. C.; Kennan, R. P.; Schulz, R. J. Magn Reson Imaging 1993, 11, 253.
14. Maryañski, M. J.; Schulz, R. J.; Ibbott, G. S.; Gatenbury, J. C.; Xie, J.; Horton, D.; Gore, J. C. Phys Med Biol 1994, 39, 1437.
15. Keall, P.; Baldock, C. Med Phys 1998, 25, A194.
16. Keall, P.; Baldock, C. Australas Phys Eng Sci Med 1999, 22, 85.
17. Maryañski, M. J.; Ibbot, G. S.; Eastman, P.; Schulz, R. J.; Gore, J. C. Med Phys 1996, 23, 699.
18. Audet, C.; Duzenli, C.; Kwa, W.; Tsang, V.; Mackay, A. Med Phys 1996, 23, 803.
19. Ibbott, G. S.; Bova, F. J.; Maryañski, M. J.; Zhang, Y.; Holcomb, S. D.; Avison, R. G.; Meeks, S. L. Med Phys 1996, 23, 1070.
20. Ibbott, G. S.; Maryañski, M. J.; Eastman, P.; Holcomb, S. D.; Zhang, Y.; Avison, R. G.; Sanders, M. S.; Gore, J. C. Int J Radiat Oncol Biol Phys 1997, 38, 1097.
21. Baldock, C.; Hasler, C. D.; Keevil, S. F.; Greener, A. G.; Billingham, N. C.; Burford, R. P. Med Phys 1996, 23, 1490.
22. Baldock, C.; Hindocha, N.; Billingham, N. C.; Burford, R. P.; Keevil, S. F.; Procter, E. Med Phys 1996, 23, 1490.
23. Baldock, C.; Burford, R. P.; Billingham, N. C.; Wagner, G. S.; Patval, S.; Badawi, R. D.; Keevil, S. F. Phys Med Biol 1998, 43, 695.
24. Oldham, M.; Baustert, I.; Lord, C.; Smith, T. A. D.; McJury, M.; Leach, M. O.; Warrington, A. P.; Webb, S. Phys Med Biol 1998, 43, 1113.
25. Baldock, C.; Rintoul, L.; Keevil, S. F.; Pope, J. M.; George, G. A. Phys Med Biol 1998, 43, 3617.
26. Gore, J. C.; Ranade, M.; Maryañski, M. J.; Schulz, R. J. Phys Med Biol 1996, 41, 2695.
27. Hilts, M.; Audet, C.; Duzenli, C. Med Phys 1999, 26, 1430.
28. Schmidt-Rohr, K.; Spiess, H. W. Multidimensional Solid-State NMR and Polymers; Academic: London, 1994.
29. Murry, P. J.; Baldock, C. Australas Phys Eng Sci Med 2000, 23, 44.
30. Földiák, G., Ed. Radiation Chemistry of Hydrocarbons; Elsevier: Amsterdam, 1981.
31. Flory, P. J. Principles of Polymer Chemistry; Cornell University Press: Ithaca, NY, 1953.
32. Chambers, K. W.; Collinson, E.; Dainton, F. S.; Seddon, W. A.; Wilkinson, F. Trans Faraday Soc 1967, 63, 1699.
33. Baldock, C.; Fitchew, R.; Murry, P. J.; Murry, M.; Back, P.; Kron, T. Med Phys 1999, 26, 1130.
34. Baldock, C.; Lepage, M.; Rintoul, L.; Murry, P. J.; Whittaker, A. K. In Proceedings of the 1st International Workshop on Radiation Therapy Gel Dosimetry; Schreiner, L. J., Ed.; Canadian Organization of Medical Physicists: Edmonton, Canada, 1999.
35. McJury, M.; Oldham, M.; Leach, M. O.; Webb, S. Phys Med Biol 1999, 44, 1863.
36. Chapiro, A. Radiation Chemistry of Polymeric Systems; Interscience Publishers: New York, 1962.
37. Haraldsson, P.; Nydén, M.; Bäck, S. Å. J.; Olsson, L. E. In Proceedings of the 1st International Workshop on Radiation Therapy Gel Dosimetry; Schreiner, L. J., Ed.; Canadian Organization of Medical Physicists: Edmonton, Canada, 1999.
38. Miyoshi, T.; Takegoshi, K.; Hikichi, K. Polym J 1994, 26, 485.
39. Rajamohanan, P. R.; Ganapathy, S.; Ray, S. S.; Badiger, M. V.; Mashelkar, R. A. Macromolecules 1995, 28, 2533.
40. Ganapathy, S.; Ray, S. S.; Rajamohanan, P. R.; Mashelkar, R. A. J Chem Phys 1995, 103, 6783.
41. Nieto, J. L.; Baselga, J.; Hernández-Fuentes, I.; Llorente, M. A.; Piérola, I. F. Eur Polym J 1987, 23, 551.
42. Eastoe, J. E.; Leach, A. A. In The Science and Technology of Gelatin; Ward, A. G., Courts, A., Eds.; Academic: London, 1977; Chapter 3.
43. O'Donnell, J. H.; Sangster, D. F. Principles of Radiation Chemistry; Edward Arnold: London, 1970.
44. Richards, E. G.; Lecanidou, R. In Electrophoresis and Isoelectric Focusing in Polyacrylamide Gels; Allen, R. C., Maurer, H. R., Eds.; de Gruyter: Berlin, 1974.
45. Gelfi, C.; Righetti, P. G. Electrophoresis 1981, 2, 220.
46. Cohen, Y.; Ramon, O.; Kopelman, I. J.; Mizrahi, S. J. Polym Sci B Polym Phys 1992, 30, 1055.
47. Bansil, R.; Gupta, M. K. Ferroelectrics 1980, 30, 63.
48. Inoue, Y.; Fukutomi, T.; Chûjô, R. Polym J 1983, 15, 103.
49. Hikichi, K.; Ikura, M.; Yasuda, M. Polym J 1988, 20, 851.
50. Maryañski, M. J.; Audet, C.; Gore, J. C. Phys Med Biol 1997, 42, 303.
51. Baselga, J.; Llorente, M. A.; Hernández-Fuentes, I.; Piérola, I. F. Eur Polym J 1989, 25, 471.
52. Callaghan, P. T. Principles of Nuclear Magnetic Resonance Microscopy; Clarendon Press: Oxford, UK, 1991.
53. Audet, C. PhD Dissertation, McGill University, Montreal, 1995.
54. Baldock, C.; Murry, P.; Kron, T. Phys Med Biol 1999, 44, N243.
55. Baldock, C.; Lepage, M.; Jayasekera, M.; Bäck, S. Å. J., unpublished results.
56. Lepage, M.; Whittaker, A. K.; Rintoul, L.; Bäck, S. Å. J.; Baldock, C., unpublished results.
57. Lepage, M.; Whittaker, A. K.; Baldock, C., unpublished results.